

ISSN 0029-3865

CONSELHO NACIONAL DE DESENVOLVIMENTO CIENTÍFICO E TECNOLÓGICO - CNPq

CENTRO BRASILEIRO DE PESQUISAS FÍSICAS - CBPF

Coordenação de Documentação e Informação Científica - CDI

Área de Publicações

CBPF-NF-061/83

X-RAY STUDY OF THE ROTATOR PHASES OF PARAFFINS

$C_{27}H_{56}$, $C_{28}H_{58}$, $C_{29}H_{60}$, $C_{30}H_{62}$, $C_{32}H_{66}$, and $C_{34}H_{70}$

by

J. Doucet, I. Denicoló, A.F. Craievich and C. Germain

Rio de Janeiro

CBPF

1983

ABSTRACT

X-ray investigations performed on the rotator phases of n-alkanes C_nH_{2n+1} with $26 \leq n \leq 34$ prove that their structures are different from those exhibited by lower-numbered compounds. Two kinds of phases with monoclinic and triclinic symmetries are encountered, both with the molecules tilted with respect to the layer plane. The inter-layer stacking modes are compared to those found in thermotropic liquid crystals.

Key-words: Paraffins; X-ray diffraction Phase transitions; Rotator phases.

I. INTRODUCTION

This paper is devoted to the structure of the rotator phase of n-paraffins (C_nH_{2n+2}) with n ranging from 27 to 34. It is a continuation of the three previously published papers (1) (2) (3) which covered n values ranging from 17 up to 26. From these studies we get evidence for the existence of two types of rotator phases, R_I and R_{II} and not only one as commonly believed up to now.

In summary the rotator phases R_I and R_{II} are characterized by a layered structure with the long molecular axes perpendicular to the layer planes. Within each layer the axes are distributed at the nodes of a periodic lattice which is rectangular centered (pseudo-hexagonal) for the R_I phase or strictly hexagonal for the R_{II} phase. In a recent work (4) Ungar studied paraffins with n ranging from 11 to 25. Its results concerning the shorter molecules prove that the orthorhombic cell of the R_I phase is F-centered and not C-centered as proposed before (1,2,3). This result also modifies the conclusions concerning the intralayer packing and molecular disorder. The phases R_I and R_{II} also differ by their layer packing. In the R_I phase the molecular axes of a upper layer are located on the centers of the losanges formed by four axes of the lower layer (fig 1-a) which leads to a ABAB packing mode characterized by an orthorhombic F-centered cell. In the R_{II} phase the molecular axes of a upper layer are located on the centers of three of the six triangles of the lower layer (fig 1-b) leading to a ABCABC packing mode which can be described by a rhomboedral cell (4).

Odd-numbered compounds C_nH_{2n+2} with n = 17, 19 and 21 exhibit a R_I phase. Odd-numbered compounds n = 23 and 25

exhibit successively the two phases R_I and R_{II} . Even-numbered compounds $n = 22, 24$ and 26 exhibit a R_{II} phase. The transition $R_I \rightleftharpoons R_{II}$ is weakly first order and is announced by large opposite amplitude variations of the lattice parameters a and b of the rectangular centered lattice parallel to the layer plane, in such a way that the ratio a/b increases with temperature up to values close to $\sqrt{3}$ which correspond to the hexagonal cell. For compounds $n = 17, 19$ and 21 the melting occurs before this value is reached.

The behavior of the lattice parameters also depends on n . For instance the value of a/b just after the transition crystal $\rightarrow R_I$ increases with n and it was expected according to this variation that compound $n = 27$ would directly give a R_{II} phase (2) whereas even-numbered compounds were also expected to give a R_{II} phase. Thus we planned to examine odd and even-numbered compounds with $n > 26$.

Even-numbered compounds $C_{28}H_{58}$ (octacosane), $C_{30}H_{62}$ (triacontane), $C_{32}H_{66}$ (dotriacontane) and $C_{34}H_{70}$ (tetratriacontane) were purchased from Fluka with the following purity grade respectively : $>98\%$, $>97\%$, 99% and $>97\%$. Compound $C_{29}H_{60}$ (nonacosane) was purchased from Serlabo and we synthesized compound $C_{17}H_{56}$ (heptacosane) by reduction of the 14-heptacosane (Clemmensen's reaction). No further purification was performed excepted for $C_{27}H_{56}$ by column chromatography. Table I gives our experimental transition temperature (measured by DTA) compared with the transition temperatures of very pure compounds (5). Compounds $n = 28, 30$ and 34 have a good purity, compounds $n = 32$ and 27 are less pure and compound $n = 29$ seems to be of low purity. Nevertheless we think that only the transition temperature are altered and not the nature of the rotator phases.

The crystallographic data have been deduced from X-ray powder diagrams recorded on a Guinier camera using the crystal reflected monochromatic beam $\text{CuK}\alpha_1$ (1.5403 Å). From these diagrams we have calculated the cell dimensions as a function of temperature.

II. RESULTS

1. Crystalline phases

The cell dimensions and the space group of the crystalline phases of the odd-numbered compounds ($n = 27$ and $n = 29$) are the same as for lower n compounds (1) (2) except for c (perpendicular to the layers) which of course is directly related to the molecular length. These results are in agreement with A. SCHAERER et al data (6). The crystal-crystal phase transitions γ and δ mentioned by G. SNYDER (7) do not seem to be accompanied by discontinuities in the variation of the cell dimensions versus temperature.

The crystalline phases of even-numbered compounds are more complicated. We have not systematically studied these crystalline phases since we were mainly concerned with the rotator phases. Nevertheless we can point out that the unit cells of compounds $n = 28, 30$ and 34 are monoclinic. For compound $n = 32$ the symmetry is orthorhombic up to 61°C and then monoclinic. This can be attributed to a lack of purity of that compound. A similar phenomena has been reported for $\text{C}_{36}\text{H}_{74}$ (8).

X-ray patterns of $\text{C}_{28}\text{H}_{58}$ performed on monodomains prove that the periodicity in the molecular axis direction is twice the molecular length and not only one time as commonly believed.

2. Rotator phases

The X-ray diagrams of the rotator phases of paraffins $\text{C}_n\text{H}_{2n+2}$ with $27 \leq n \leq 34$ could not be indexed neither with orthorhombic (R_I) nor hexagonal (R_{II}) cells. The compounds

$n = 27, 29$ and 30 exhibit successively two phases R_{III} and R_{IV} , the R_{III} phase being the low temperature one. Even-numbered compound $n = 28$ exhibits a R_{IV} phase and compounds $n = 32$ and 34 a R_{III} phase. Typical powder diagrams of phases R_{III} and R_{IV} are shown on figure 2. Bragg reflections on layers (not shown on the figure) are also visible on both diagrams at low diffraction angles. At large diffraction angles a few weak and diffuse bands appear, the position of which is difficult to ascertain with precision.

The R_{III} phase patterns (fig 2-a) exhibit three intense rings corresponding to very close reticular distances and having comparable intensities differing by less than a factor three. Others sharp and weak diffraction rings are also visible between the three main rings and at slightly larger angles too (see table II). As for all rod-shaped molecules packed in a layer structure with pseudo-hexagonal order of the molecular axes within the layers, the intense diffraction rings proceed from the three fundamental reticular distances (100) , (010) and $(\bar{1}10)$. Since the three reticular distances are different for the R_{III} phase, we can conclude that the R_{III} phase is characterized by a triclinic unit cell.

As regards the R_{IV} phase only two intense rings are visible (fig 2-b), the inner one being about five times more intense than the other. This type of pattern can be explained either by an orthorhombic unit cell or by a monoclinic unit cell. The presence of a few weak diffraction rings at lower angles than the first intense ring eliminates the possibility of the orthorhombic cell. Thus the R_{IV} phase is characterized by a monoclinic unit cell. We must mention that the weak rings are not always visible, which implies that we have not a definite proof of a monoclinic symmetry for $C_{28}H_{58}$ and $C_{30}H_{62}$. Nevertheless this assumption is highly probable because in the case of an orthorhombic symmetry the inner ring is about two times more intense than the other.

Unfortunately the exact unit cell dimensions of R_{III} and R_{IV} phases cannot be determined because of the small number of diffraction rings and of the lack of precision of the large angle diffraction rings. A large number of unit cells account for the position of the diffraction rings within the experimental error. Nevertheless they exhibit a few common features which are meaningful for the understanding of the molecular packing. A few comments can be done :

- i/ the structures are single layer structures but reflections (00ℓ) with ℓ odd are much weaker than the others which indicates that the structure is close to a bilayer structure. Contrarily to the R_I and R_{II} phases, the molecular axes in the R_{III} and R_{IV} phases are tilted with respect to the normal to the layers, the tilt angle being included in the range $(0^\circ-15^\circ)$. The c length can be smaller or equal to the most elongated molecular length. We found instructive the comparison between the layer thickness d and the theoretical molecular length calculated in the t-t-t configuration using datas of ref (9) and (10). On figure 3 is represented the variation of $(d - \ell)$ as a function of n . From $n = 17$ to $n = 25$ this difference slowly increases up to zero and then abruptly decreases down to $- 2.5 \text{ \AA}$ for $n = 33$ or $n = 34$. The increasing part of the variation can be explained by a decrease of the "layer interpenetration" while the decreasing part either means that the tilt angle increases with n or is relevant of a molecular length shortening due to the presence of systematic chain defects (both effects are also possible) ;
- ii/ the lattice within the layers is pseudo-hexagonal for the R_{III} and R_{IV} phases. The dimensions of the rectangular (R_{IV} phase) or pseudo-rectangular (R_{III} phase) centered cells are similar to those encountered in the R_I and R_{II} phases. The area per molecules ($\sim 19.8 \text{ \AA}^2$) seems equal or slightly larger than the area in the R_{II} phase (19.6 \AA^2) ;

iii/ the position of the powder rings changes with temperature. The effect is too large to be only due to a classic thermal expansion. As for the orthorhombic R_I phase the geometry of the triclinic cell of the R_{III} phase undergoes a continuous transformation which is relevant of a structural change. The R_{III} cell seems to gradually transform into the R_{IV} cell since the two first intense rings get closer when the temperature increases.

III. DISCUSSION

It is not the first time that a triclinic symmetry is found for a rotator phase since W. PIESCZEK et al (11) showed that the rotator phase of compound $C_{33}H_{68}$ is triclinic. It is reasonable to assume that this triclinic phase is a R_{III} phase type. But it is the first time to our knowledge that a rotator phase R_{IV} is described with a monoclinic symmetry.

No coexistence of the two phases has been observed at the phase transition $R_{III} \rightarrow R_{IV}$ on the X-ray patterns and we already mentioned that the R_{III} unit cell gradually transforms into the R_{IV} unit cell. D.S.C. scans show at the $R_{III} - R_{IV}$ transition temperature a very small reproducible thermal anomaly involving an energy lower than 2 cal/mole. This anomaly is neither typical of a first order transition nor of a second order transition.

The (T, n) phase diagram, shown in figure 4, has some interesting features. In order to obtain a coherent diagram independent of the purity grade of the sample we have plotted the temperatures of pure compounds (5). For the $R_{III} \rightarrow R_{IV}$ transition we have respected the value of the temperature range of the R_{III} phase. It is clear that the $R_{III} \rightarrow R_{IV}$ phase transitions delimit a curve (A) above which the rotator phase is of the R_{IV} type. This curve A

passes exactly at the crystal \rightarrow rotator transition temperature of $C_{28}H_{58}$, which explains that this compound directly transforms into a R_{IV} phase (on cooling down a supercooled R_{III} phase is exhibited). As no data is available for $C_{31}H_{64}$ we only can say that the curve A becomes higher than the (rotator \rightarrow liquid) curve between $n = 30$ and $n = 32$. The curve A delimiting the R_{III} and R_{IV} regions for compounds $n > 26$ is quite similar to the curve B delimiting the R_I and R_{II} regions for compounds $n \leq 26$.

The phase transition $R_{III} \rightarrow R_{IV}$ as well as the $R_I \rightarrow R_{II}$ exhibit similar features to the liquid crystal phase transitions displayed by alkoxybenzylidene compounds : freely suspended thick films of hexpyloxybenzylidene-hexpylaniline evolves when decreasing temperature from a hexagonal close-packed structure (ABAB packing) through intermediate orthorhombic F and monoclinic phases, to a simple hexagonal structure (12). These transitions can be viewed as restacking transitions of adjacent layers characterized by a pseudo-hexagonal or hexagonal distribution of the molecules axes. The same approach can be used for the four rotator phases. Figure 5 shows the corresponding interlayer packing modes. The $R_I \rightarrow R_{II}$ transition involves a layer displacement of $\frac{1}{6} \vec{a}$; the displacement at the $R_{III} \rightarrow R_{IV}$ transition is not known since the unit cell are not exactly determined.

As for liquid crystals, these restacking transitions are accompanied by intralayer rearrangements concerning the cell dimensions, the tilt angle and probably also the molecular motions. But it is not known whether the restacking transitions induce intralayer rearrangements or if it is the contrary. It is worth noting that the restacking transitions are generally associated to very weak thermal effects.

The exact nature of the factors governing the restacking transitions in paraffins remains mysterious. The complicated phase diagram (T, n) of the crystalline phases of odd-numbered compounds proves the existence of several competing forces, the leadership of which can be changed with both n and T. The same conclusion also applies for even-numbered compounds. The number and the complexity of the factors involved in the rotator phases range is enhanced by the molecular motions and molecular deformations. It is well established now that the molecules not only undergo rotational motions around their long axes (probably coupled with longitudinal translations) but also conformational changes destroying the molecular symmetry elements of the crystalline phase (13) (14) (15). As the proportion of distorted molecules increases with n, it is possible that above some proportion the number of distorted molecules induce another "mean" molecular symmetry leading to different structures than for non-distorted molecules. For instance the disappearance of the mirror plane perpendicular to the long axis allows a structure with tilted molecules. This explanation of the different features of rotatory phases for paraffins with n above and below 26 is quite hypothetical. Complementary experiments, mainly concerning the molecular dynamics, are needed to better understand the phase behavior of paraffins.

TABLE I

n	C → R		R → L	
	T _{lit}	T _{mes}	T _{lit}	T _{mes}
27	52.6	51.6	58.4	57.8
28	57.6	57.8	60.8	60.8
29	57.8	55.9	63.	60.5
30	61.6	61.6	65	64.9
32	65.1	64.2	68.9	68.7
34	69.0	69.2	72.7	72.3

Comparison between literature values of transition temperature (5) and experimental values of measured by D.T.A. (in °C) at the crystalline → rotator (C → R) and rotator → liquid (R → L) transitions

TABLE II

R _{III} (53°C)			R _{IV} (58°C)		
36.3	±0.1	+	36.5	±0.1	+
24.1	±0.1	+	24.4	±0.1	+
12.05	±0.05	+	12.22	±0.05	+
4.193	±0.005	*	4.200	±0.005	
4.147	±0.005	*	4.166	±0.005	*
4.035	±0.005	*	4.138	±0.005	
3.932	±0.005		4.111	±0.005	
2.44	±0.02	d	4.087	±0.005	*
2.38	±0.02	d	2.43	±0.02	d
			2.36	±0.02	d

Reticular distances in Å measured in the R_{III} and R_{IV} phases of C₂₇H₅₆. + layer reflexion ; * intense ring ; d diffuse ring.

REFERENCES

- (1)- J. Doucet, I. Denicolò, A.F. Craievich, J. Chem. Phys., 75 (3), 1523 (1981).
- (2)- J. Doucet, I. Denicolò, A.F. Craievich, A. Collet, J. Chem. Phys., 75 (10), 5125 (1981).
- (3)- I. Denicolò, J. Doucet, A.F. Craievich, J. Chem. Phys., 78 (3), 1465 (1983).
- (4)- G. Ungar, J. Phys. Chem., 87, 689 (1983).
- (5)- M.G. Broadhurst, J. Res. Nat. Bur. Stand., 66A (3), 241 (1962).
- (6)- A.A. Schaerer, C.J. Busso, A.E. Smith, L.B. Skinner, J. Am. Chem. Soc., 77, 2017 (1955).
- (7)- R.G. Snyder, M. Maroncelli, Song Ping Qi, H.L. Strauss Science, 214, 188 (1981).
- (8)- H.M.M. Shearer, V. Vand, Acta Cryst., 9, 379 (1956).
- (9)- M. Kobayashi, H. Tadokoro, Macromolecules, 8, 897 (1975).
- (10)- M. Kobayashi, J. Chem. Phys., 68 (1), 145 (1978).
- (11)- W. Piesczek, G.R. Strobl, K. Malzahn, Acta Cryst., B30, 1278 (1974).
- (12)- J. Collett, L.B. Sorensen, P.S. Pershan, J.D. Litster, R.J. Birgeneau, Phys. Rev. Lett., 49 (8), 553 (1982).
- (13)- M. Maroncelli, Song Ping Qi, H.L. Strauss, R.G. Snyder, J. Am. Chem. Soc., 104, 6337 (1982).
- (14)- G. Zerbi, R. Magni, M. Gussoni, K.H. Moritz, A. Bigotto, S. Dirlokov, J. Chem. Phys., 75 (7), 3175 (1981).
- (15)- B. Ewen, E.W. Fischer, W. Piesczek, G. Strobl, J. Chem. Phys., 61 (12), 5265 (1974).

FIGURE CAPTIONS

-
- Fig 1 - Relative molecular positions between neighbouring layers.
- 1-a In the R_I phase there are two different positions (packing ABAB).
- 1-b In the R_{II} phase there are three different positions (packing ABCABC).
- Fig 2 - Microdensitometer profile of the powder patterns of $C_{29}H_{60}$, in the R_{III} and R_{IV} phases in the range $(4.6 - 3.6) \text{ \AA}$.
- Fig 3 - Plot of $(d - \lambda)$ versus n where d is the experimental thickness of one layer and λ the theoretical molecular length in its most elongated conformation. The point $n = 33$ is given by ref. 11.
- Fig 4 - Phase diagram (T, n) showing the different rotator phase regions.
- Fig 5 - Relative molecular positions between two adjacent layers ; the empty circles correspond to the reference layers. $\vec{\delta}_1$ corresponds to the displacement at the $R_I^{(F)} \rightarrow R_{II}^{(R)}$ phase transition and $\vec{\delta}_2$ corresponds to one possible displacement at the $R_{III}^{(T)} \rightarrow R_{IV}^{(M)}$ phase transition since in that case the positions for R_{III} and R_{IV} are not precisely known.

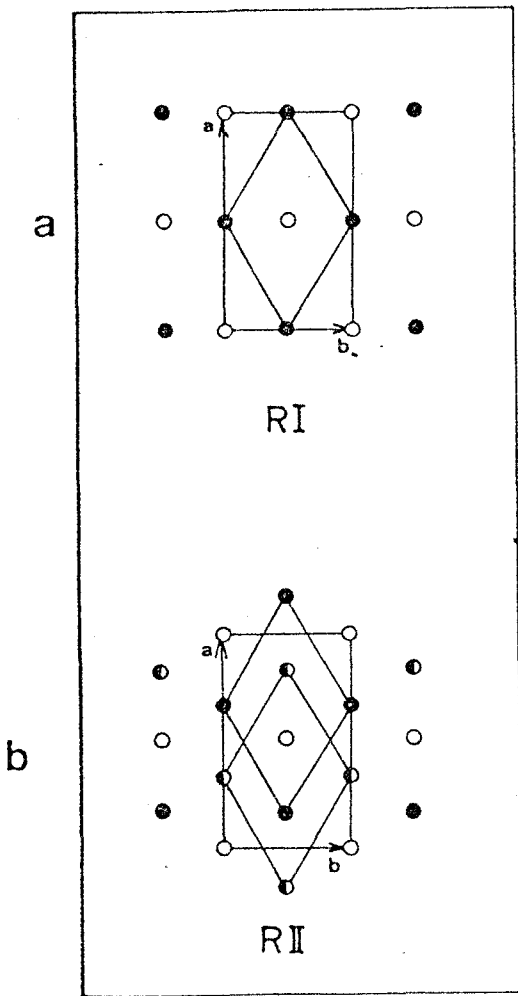


Fig. 1

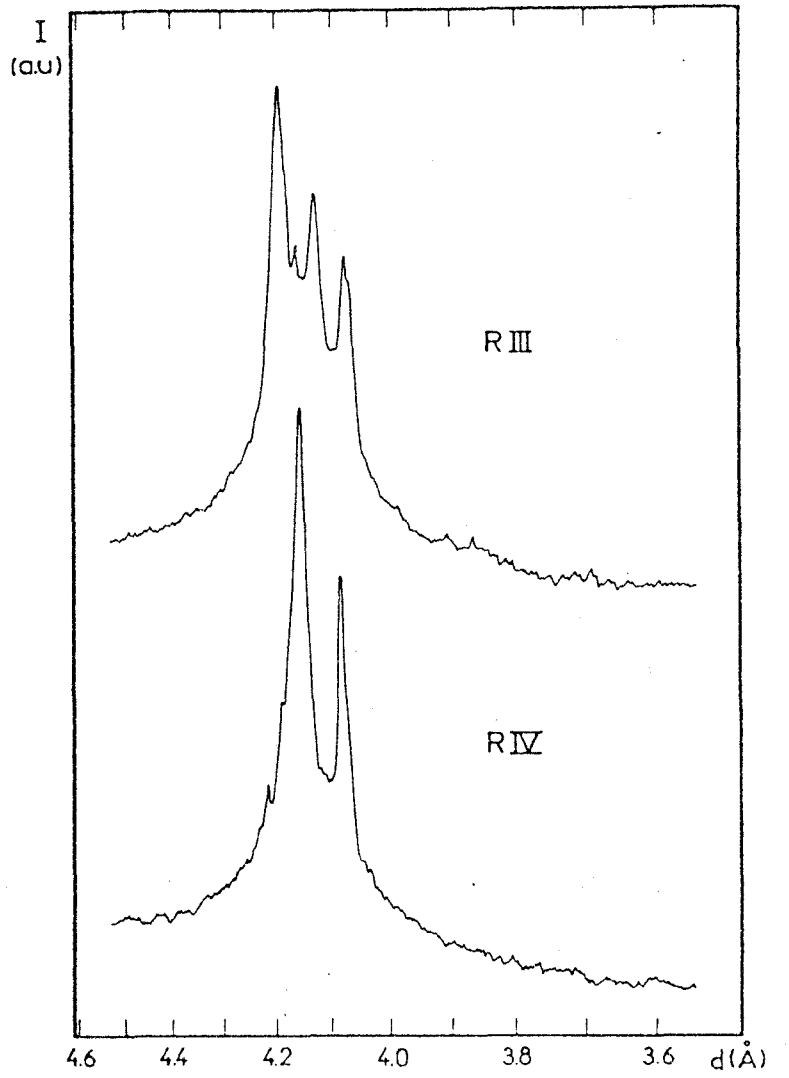


Fig. 2

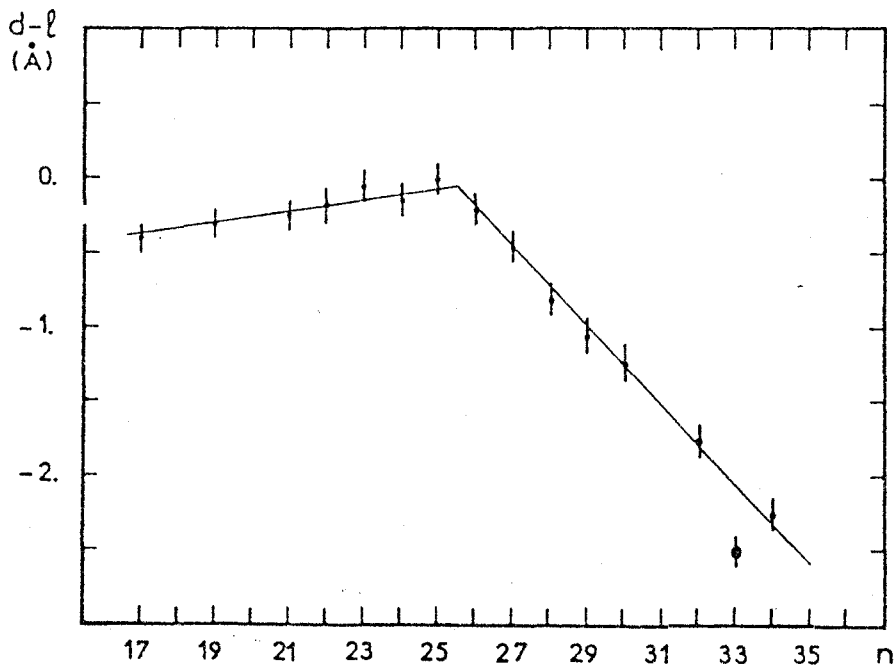


Fig. 3

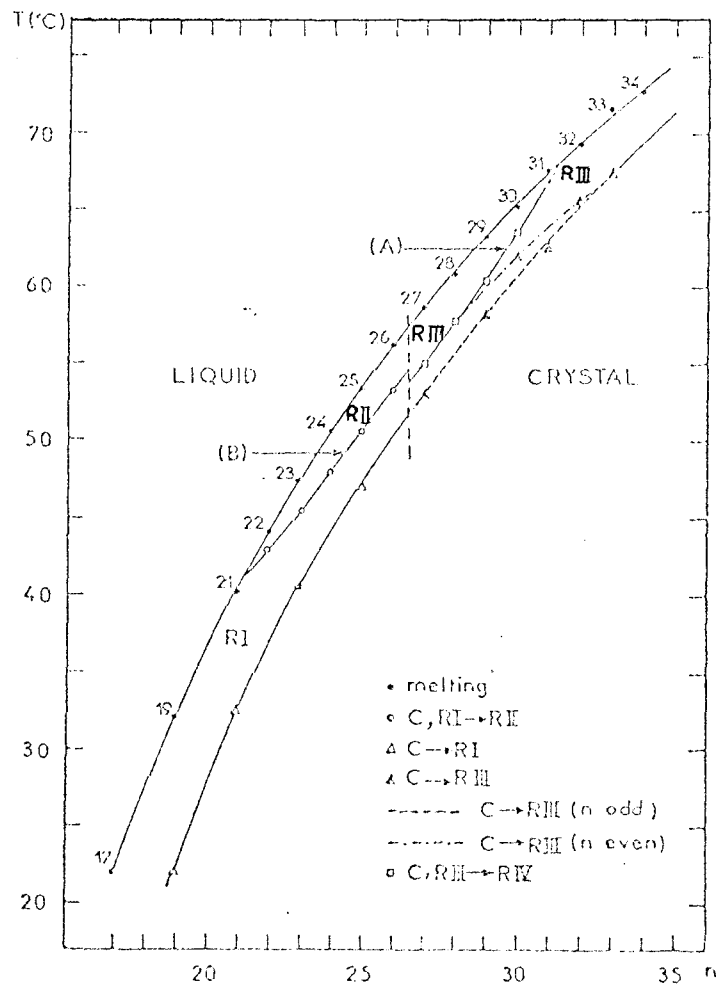


Fig. 4

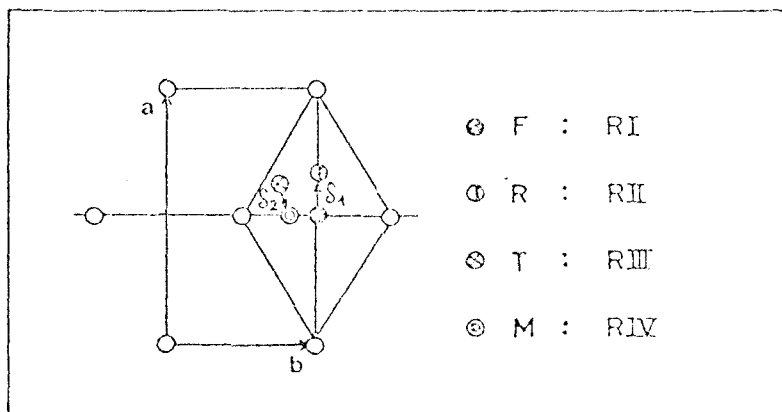


Fig. 5